PERGAMON

Journal of Geodynamics 31 (2001) 411–428

JOURNAL OF GEODYNAMICS

www.elsevier.nl/locate/jgeodyn

Small-scale structure of lithosphere-asthenosphere beneath Gauribidanur Seismic array deduced from amplitude and phase fluctuations

Jayant N. Tripathi

Department of Earth and Planetary Sciences, University of Allahabad, Allahabad-211 002, India

Received 30 December 1999; received in revised form 12 September 2000; accepted 10 February 2001

Abstract

The cross coherence function between log amplitude and phase (or travel time) has been analyzed along with the transverse coherence functions of log amplitude and phase in order to estimate the statistical distribution of heterogeneities beneath the Gauribidanur Seismic array (GBA). The power spectra of the P-wave velocity variations can be estimated under the array with the help of the transverse coherence functions (TCFs). The data of 72 earthquakes have been used to calculate the three TCFs (of phase, log amplitude and cross-coherence). The central frequency is 2 Hz. The measured root mean square (rms) log amplitude fluctuation is 0.40 and the rms phase fluctuation is 0.88. An overlapping two-layer model has been obtained for lithosphere and asthenosphere heterogeneities beneath GBA with different power law spectra. The upper layer, in which the heterogeneities are defined by Gaussian correlation function extends from the surface to about 160 km depth while the lower layer, in which the heterogeneities are defined by exponential correlation function extends from 16 to 280 km. The rms P-wave velocity variation has been estimated in the range of 0.3–1.5%. Clustering of cracks or intrusions may be responsible for the small-scale heterogeneities while temperature or compositional heterogeneities may be the cause of large-scale wave heterogeneities.

Keywords: GBA; Heterogeneities; rms; Scattering; Transverse coherence functions

1. Introduction

It is known that the earth is laterally inhomogeneous from the crust, mantle to the core. The change in the seismic waveform, travel-time (or phase) and amplitude fluctuations as well as

E-mail address: jntripa@yahoo.com

0264-3707/01/$ - see front matter
PII: S0264-3707(01)00007-2

apparent attenuation of direct arrivals may be due to the velocity and density heterogeneities of the medium. In other words, the seismic waves are distorted, scattered, diffracted and become somewhat irregular in a medium with random heterogeneities. The seismic waves sensitive to the different effects are the causes of different scale-length to these inhomogeneities. The geodynamical processes of the earth may have introduced these heterogeneities. The seismic wave scattering, which is modification of seismic waves due to heterogeneities, can be considered as random and some statistical properties of the medium and parameters of its heterogeneities can be deduced. Thus, understanding the nature of the heterogeneities of the earth may give clues to the geodynamical process of the earth responsible for the generation of these heterogeneities.

Statistical characteristics of small-scale structure in the earth have been determined by direct P-wave amplithde and time fluctuations (Aki, 1973; Capon, 1974; Capon and Berteussen, 1974; Berteussen et al., 1975, 1977; Powell and Meltzer, 1984; Tripathi and Ram, 1996), coda strength (Aki, 1981; Sato, 1982; Wu and Aki, 1985a,b,c) and attenuation by scattering (Aki and Chouet, 1975; Aki, 1980; Wu, 1982; Sato, 1982). The variances of log-amplitude and phase and covariance of log-amplitude and phase have been used previously (Aki, 1973; Capon, 1974; Capon and Berteussen, 1974; Berteussen et al., 1975, 1977; Powell and Meltzer, 1984; Tripathi and Ram, 1996).

The modern theory of wave propagation through random media (WPRM) began with the perturbation techniques or propagation though weak fluctuation (Bergmann, 1946; Mintzer, 1953; Chernov, 1960; Tatarskii, 1971) using Born approximation, The assumption was made that the medium was characterized by the Gaussian correlation function, but unfortunately, no natural medium is known with this property. The parabolic equation method was used where it is assumed that the waves are concentrated within a small angular region around the direction of propagation. A great advantage of this method is line integrals along deterministic rays, rather than volume integrals in the formula. Using the parabolic equation method a theory for wave propagation through homogeneous isotropic turbulent media was developed and a power law spectrum was also obtained for these media (Tatarskii, 1971; Prokhorov et al., 1975; Ishimaru, 1977; Fante, 1980; Tatarskii and Zavorotnyi, 1980; Strohbehn, 1978). For P-wave signals, the full wave scattering problem has been solved with the help of the parabolic wave equation and successfully used to estimate the velocity perturbations and extension of the heterogeneous media at the Norwegian Seismic Array (NORSAR) (Flatte and Wu, 1988; Wu and Flatte, 1990). These authors also used the transverse cross-coherence functions between arrival time and log-amplitude and angular coherence functions for their study. They have interpreted that the heterogeneities can be represented by two overlapping-layers with different type of random heterogeneities. Finally, the reliability of this two over-lapping layer model has also been established (Flatte et al., 1991).

Weak-scattering theory has been applied to P wave teleseismic propagation. It is assumed that the waves arriving at a few hundred kilometers below an array, like the Gauribidanur Seismic array (GBA) (Fig. 1) are essentially in plane waveform. Any effect due to inhomogeneities near the source is too large to be observed by a 32 km aperture array and any effect due to very deep mantle heterogeneity has no significant effect on the wave with scale lengths less than the 32-km size array. The inhomogeneities near the source have little effect due to two reasons. Firstly, only a very small range of initial angles at the source is seen by the array and secondly, the spreading of the ray tube magnifies any small-scale fluctuations of the wave front into large-scale fluctuations at the

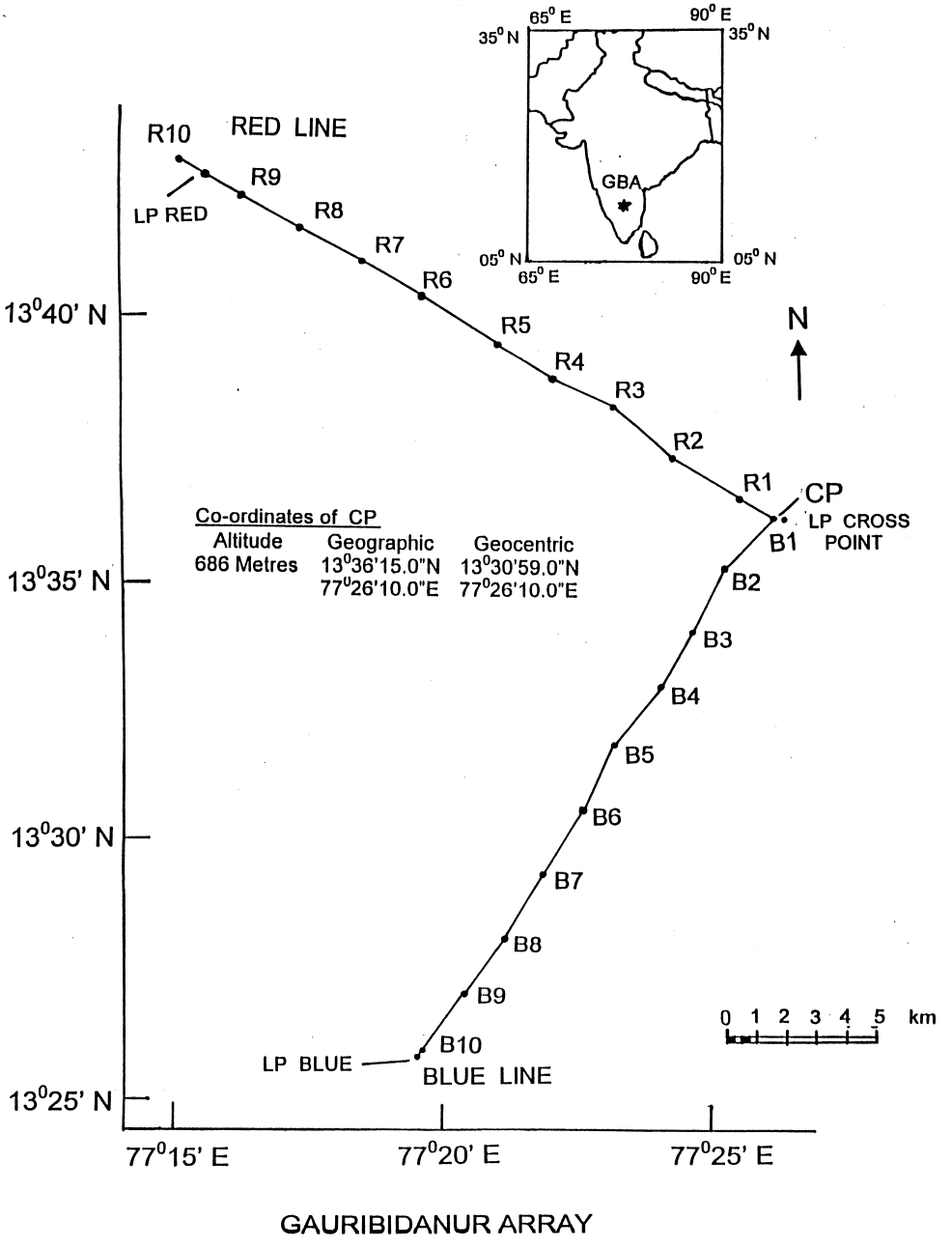

Fig. 1. Location and configuration of the Gauribidanur medium aperture seismic array.

receiver. It is also assumed here that wave scattering within a reasonably narrow cone due to inhomogeneities within a few hundred kilometers depth below the array is the cause for the arrival time and amplitude fluctuation. It is also realized that the first few seconds of P wave arrivals represent scattering at small angles; however, coda can be restricted to scattering at large angles.

In this paper, a two-overlapping-layer model has been evaluated on the basis of wave propagation theory through random media. In this model, the heterogeneities of the layers are defined with different type of correlation function. Small-scale structures in the lithosphere and asthenosphere have been deduced from the travel time and amplitude fluctuations at GBA. These heterogeneities may be introduced by the mantle convection. The rms velocity perturbations are also estimated for the layers of the given model.

2. Theory of wave propagation through random media based on parabolic equation method

Let the wave function arriving at the centre of the array be

$$U = U_0 \ e^{\psi} \tag{1}$$

where U_0 is the wave function that would arrive in the absence of random inhomogeneities. Then the perturbation quantity ψ can be found as given below;

$$\psi = \Delta u + i\Delta\phi \tag{2}$$

where log-amplitude is defined as u and ϕ is the phase.

It is known that for weak-scattering case confined to a narrow cone of $1/ka$, where k is wavenumber and a is scale-length, in an intrinsically dispersive-free medium, the phase fluctuations can be defined in terms of arrival time fluctuations τ and angular frequency ω, such as:

$$\phi = \omega\tau \tag{3}$$

It is assumed that the random medium is horizontally homogeneous i.e. the spectrum is independent of horizontal position. The three-dimensional wave number $\mathbf{K}$ can be split into its three components as $\bar{K} = (K_x, K_y, K_z)$ in x, y, z directions, respectively. K_x and K_y can be represented by the two-dimensional vector $\mathbf{K}_T$ transverse to the z direction; i.e. $\mathbf{K}_T$ is in the x–y plane. Thus, the spectrum of the random medium can be written as;

$$W(\mathbf{K}, z) = W\big(K_x, K_y, K_z, z\big) = W(\mathbf{K}_T, K_z, z) \tag{4}$$

The transverse coherence of fluctuations can be measured as a function of transverse separation $\mathbf{r}_T$ for plane wave incidence. Then the transverse coherence functions (TCFs) for log-amplitude (u_1, u_2), phase (ϕ_1, ϕ_2) and their cross-coherence (u_1, ϕ_2) can be written (Munk and Zachariasen, 1976; Flatte et al., 1979; Flatte and Wu, 1988; Flatte and Moody, 1990; Wu and Flatte, 1990). Since horizontal homogeneity of the spectrum is assumed, these fluctuations depend only on the difference between the two positions. The horizontal isotropy of the spectrum is also assumed; that is, $W(\mathbf{K}_T, 0, z)$ is independent of the direction of $\mathbf{K}_T$ and depends only on the magnitude of $\mathbf{K}_T$. Thus, the $\mathbf{K}_T$ integrals may be expressed in polar coordinates and the angular integrals may be taken. Thus, the resultant expressions will be function of magnitude of separation (r_T) only and not direction:

$$\langle u_1(r_T)u_2(0)\rangle = 4\pi^2k^2\int_0^L \mathrm{d}z\int_0^\infty k_T\mathrm{d}k_T J_0(k_T.r_T)\sin^2\left(\frac{k_T^2 z}{2k}\right)W(k_T, 0, z) \tag{5}$$

$$\langle \phi_1(r_T)\phi_2(0)\rangle = 4\pi^2k^2\int_0^L \mathrm{d}z\int_0^\infty k_T\mathrm{d}k_T J_0(k_T.r_T)\cos^2\left(\frac{k_T^2 z}{2k}\right)W(k_T, 0, z) \tag{6}$$

$$\langle u_1(r_T)\phi_2(0)\rangle = 4\pi^2k^2\int_0^L \mathrm{d}z\int_0^\infty k_T\mathrm{d}k_T J_0(k_T.r_T)\sin\left(\frac{k_T^2 z}{2k}\right)\cos\left(\frac{k_T^2 z}{2k}\right)W(k_T, 0, z) \tag{7}$$

where J_0 is the zero-order Bessel function and L is the depth of deepest inhomogeneities being analyzed.

Thus, the normalized TCFs can be defined as;

$$\langle u_1(r_T)u_2(0)\rangle_N = \frac{\langle u_1(r_T)u_2(0)\rangle}{u^2} \tag{8}$$

$$\langle \phi_1(r_T)\phi_2(0)\rangle_N = \frac{\langle \phi_1(r_T)\phi_2(0)\rangle}{\phi^2} \tag{9}$$

$$\langle u_1(r_T)\phi_2(0)\rangle_N = \frac{\langle u_1(r_T)\phi_2(0)\rangle}{u_{\mathrm{rms}}\phi_{\mathrm{rms}}} \tag{10}$$

If $r_T = 0$ then these TCFs will be 1, 1 and ρ (i.e. the amplitude-phase correlation) respectively.

Normalized TCFs for a medium with an exponential correlation function with scale-length $a = 18$ km (Tripathi and Ram, 1996) are shown in Fig. 2. That is;

$$W(K) = \frac{\langle \mu^2\rangle a^3}{\pi^2}\cdot\frac{1}{(1+K^2a^2)^2} \tag{11}$$

where $<\mu^2>$ is the variance of the fractional change in the wave speed due to the random heterogeneities.

3. Seismological results

The information obtained from the variances of log-amplitude and phase can be represented in form of γ and ρ, which are defined as;

$$\gamma = u_{\mathrm{rms}}/\phi_{\mathrm{rms}} \tag{12}$$

$$\rho = \frac{\langle u\phi\rangle}{u_{\mathrm{rms}}\phi_{\mathrm{rms}}} \tag{13}$$

where $u^2_{\mathrm{rms}} = \langle u^2 \rangle$ and $\phi^2_{\mathrm{rms}} = \langle \phi^2 \rangle$. Both γ and ρ are ratios. For a medium that extends to a depth L and the fluctuation statistics are independent of the depth, the ratios γ and ρ will depend on one parameter, $D = 4L/ka^2$, called the wave parameter (Chernov, 1960). For a given a, the scale

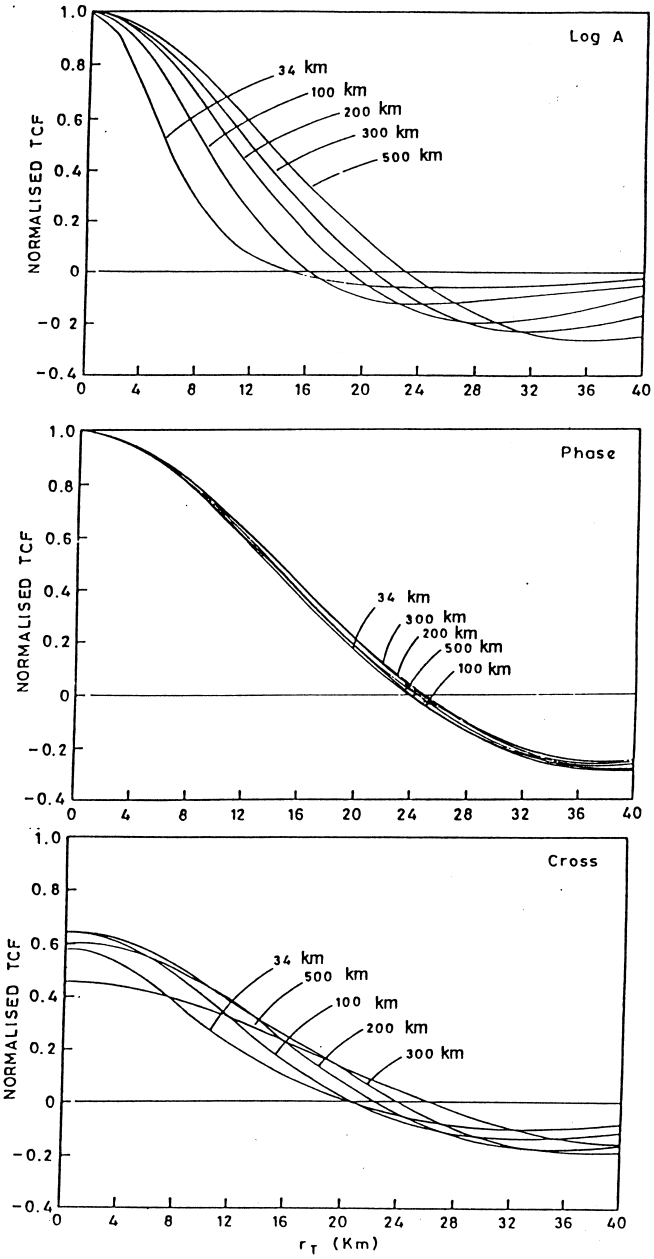

Fig. 2. The transverse coherence functions (TCFs) of log-amplitude, phase and their cross coherence, for an extended medium with an exponential correlation function. Scale length = 18 km and seismic frequency = 2 Hz. The different curves are the extension of the media from the surface to different depths in km.

length, parameter D characterizes the spectrum $W(\mathbf{K})$ of the random medium D. There will be a unique curve in γ–ρ for each type of medium spectrum (Fig. 3).

The curves for the spectrum of the Gaussian, exponential and Kolmogorov functions are shown in the Fig. 3 along with the results obtained other workers (Table 1). A comparison of results obtained from the present work (Table 1) with others is also shown in this figure. It is clear from the figure that the Gaussian spectrum does not fit the data well while the exponential and Kolmogorov spectrum are closer to the fit the data. It is seen that averages of variances are in good agreement for the power law (exponential and Kolmogorov) type of medium rather than a Gaussian spectrum while individual results are scattered. The plotted γ-ρ value of the present study lies between Gaussian and exponential spectrum. So, it is inferred that the data may be

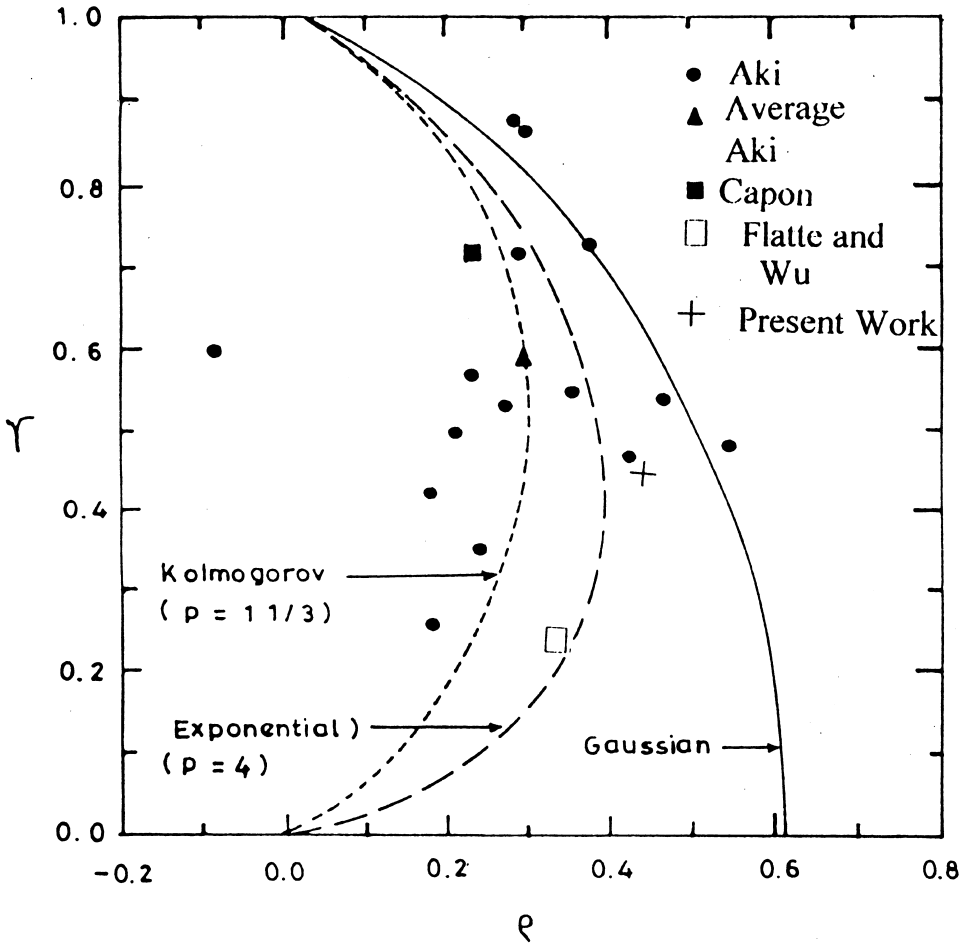

Fig. 3. Variance ratio γ verses amplitude-phase correlation ρ for uniform extended media. The solid circles are from Aki (1973). The solid square is from Capon (1974). The open rectangle is from Flatte and Wu (1988) and plus is from the present study. The quantity 'p' is spectral power law index. The data fit the power law more closely (modified after Flatte and Wu, 1988).

Table 1
A comparison of obtained values of variances

References	τ_{rms} (s)	u_{rms}	ρ
Aki (1973)	0.13	0.32	0.35
Capon (1974)	0.10	0.40	
Berteussen et al. (1975, 1977)	0.006–0.11	0.2–0.4	
Flatte and Wu (1988)	0.135	0.41	0.26
Present work	0.070	0.40	0.44

effectively explained by exponential and Gaussian correlation functions and thus a two-overlapping-layer model with these correlation functions has been considered to interpret the data.

The events recorded at GBA, which have been used in this analysis, are listed in Table 2. A frequency filter has been used to restrict the seismic frequency to 1–3 Hz, at the central frequency 2 Hz. Then the Fourier amplitude and phase have been computed for the seismograms. The TCFs for log-amplitude, phase and their cross-coherence have been computed and also normalization is done. Different possible pair combinations of seismometers have been used for the computation of TCFs of log amplitude, phase and their cross.

The TCFs are plotted against transverse separation r_T where all pairs of elements have been included with their separation r_T. The results obtained by above procedure are shown in Fig. 4. It is seen that the smallest separation available between two seismometers (R_1 and B_1, Fig. 1) is about 1.5 km and coherence for log-amplitude is about 0.6 at that separation.

4. Model of earth structure under GBA

There is a restriction placed by the nature of GBA upon the scale of earth structure that can be resolved with the array data. The maximum distance between the two sensors (R_{10} and B_{10}, Fig. 1) at GBA is approximately 32 km. The plane waves have been subtracted from the data across the array, so earth structure cannot be observed with scales larger than 32 km. The minimum distance between two sensors (R_1 and B_1, Fig. 1) is approximately 1.5 km. So, one can not observe structure with wave length smaller than 1.5 km. Furthermore, the typical seismic wavelength of 2.5 km for a frequency of 2 Hz also implies that one can not observe structure wavelength less than $\sim$2.5 km. These facts have to be taken into account in the theoretical models with which we compare the observational data.

The first model is one with an exponential correlation function with a scale length of 18 km (Tripathi and Ram, 1996), which was obtained earlier (Fig. 4). It is seen that the TCF data is not fitted to the medium variations for different depths. The disagreement at large separations are less severe than that at small separations.

The Fig. 3 indicates that there is a better fit to the data with exponential (exponent $p=4$) or Kolmogorov (exponent $p=3$) correlation function. Thus, further models can be tested having a particular type of spectrum: a power law expressed in the form;

Table 2
List of events used in the present study

S.	Date			Orig. time			Location		Delta in deg.	Az in deg.	FD in km	M
N.	d	m	y	h	min	s						
1.	11	7	72	05	54	44.1	36.384 N	70.727 E	23.47	346.3	206	5.4
2.	11	7	72	20	46	11.6	24.287 N	94.701 E	19.46	54.4	48	4.6
3.	11	1	74	02	03	50.4	36.298 N	70.772 E	23.38	346.3	159	4.8
4.	8	4	72	05	23	49.1	5.078 N	61.993 E	17.42	242.4	33	4.9
5.	8	4	72	06	42	13.3	29.674 N	89.471 E	19.49	32.9	33	4.8
6.	9	4	72	04	10	50.7	42.181 N	84.650 E	29.15	11.0	33	5.9
7.	9	4	72	08	43	48.5	40.125 N	78.830 E	26.45	2.4	14	4.7
8.	9	4	72	10	43	56.3	41.987 N	84.640 E	28.96	11.1	33	4.8
9.	9	4	72	22	47	36.8	35.127 N	74.612 E	21.58	353.7	49	4.9
10.	10	4	72	02	06	53.2	28.434 N	52.829 E	27.22	306.7	33	6.1
11.	10	4	72	02	34	31.5	28.419 N	52.909 E	27.15	306.7	33	4.9
12.	10	4	72	04	36	15.5	28.296 N	52.979 E	27.04	306.6	33	4.6
13.	10	4	72	08	33	51.8	28.253 N	53.075 E	26.94	306.6	33	4.6
14.	10	4	72	14	35	34.3	28.282 N	53.083 E	26.95	306.6	33	4.6
15.	11	4	72	06	00	04.6	7.367 N	61.996 E	27.38	332.5	33	4.9
16.	11	4	72	06	21	10.0	42.039 N	84.408 E	28.97	10.8	33	4.6
17.	12	4	72	18	37	40.8	8.321 N	53.086 E	26.97	306.7	33	5.1
18.	12	4	72	21	38	24.0	38.282 N	66.462 E	26.44	340.3	62	4.7
19.	12	4	72	23	07	49.9	28.378 N	53.035 E	27.03	306.8	33	5.0
20.	14	4	72	18	15	16.4	6.638 S	105.761 E	34.57	123.8	80	5.3
21.	16	4	72	01	27	55.7	1.844 S	99.829 E	26.99	123.0	33	5.3
22.	17	4	72	02	24	49.3	33.963 N	72.876 E	20.69	349.2	45	4.8
23.	17	4	72	10	35	45.7	25.584 N	95.358 E	20.64	52.0	108	5.0
24.	17	4	72	15	12	43.5	31.945 N	59.340 E	24.66	320.7	44	4.5
25.	18	4	72	23	22	36.4	39.971 N	51.308 E	34.88	323.7	33	4.8
26.	20	4	72	00	35	56.7	42.005 N	84.583 E	28.97	11.0	33	5.1
27.	21	4	72	21	19	29.5	34.987 N	81.033 E	21.54	8.1	33	4.8
28.	22	4	72	13	17	57.7	17.409 N	94.305 E	16.69	74.7	33	4.8
29.	23	4	72	20	40	10.0	5.742 S	104.219 E	32.81	124.2	103	5.5
30.	25	4	72	13	21	14.8	28.364 N	53.180 E	26.91	306.9	45	5.0
31.	27	4	72	05	51	06.3	.582 S	99.636 E	26.13	120.9	54	5.3
32.	28	4	72	00	52	56.8	31.259 N	84.903 E	18.87	20.1	33	5.1
33.	28	4	72	11	30	18.1	17.039 N	94.772 E	17.07	76.3	33	5.4
34.	29	4	72	16	04	21.1	28.290 N	52.965 E	27.05	306.6	33	4.9
35.	21	8	72	14	04	33.9	27.232 N	87.976 E	16.76	34.4	33	4.8
36.	21	8	72	18	55	07.1	7.229 N	88.019 E	16.78	34.5	33	5.1
37.	21	8	72	21	57	17.2	8.280 S	105.946 E	35.69	125.9	62	5.3
38.	30	8	72	15	14	09.9	6.723 N	96.472 E	28.64	33.1	33	5.5
39.	30	8	72	18	47	42.6	36.599 N	96.422 E	28.52	33.2	33	5.5
40.	2	9	72	10	37	39.4	39.882 N	53.652 E	33.5	325.8	33	4.9
41.	3	9	72	16	48	28.8	35.979 N	73.417 E	22.57	351.5	36	6.3
42.	3	9	72	17	09	18.9	35.955 N	73.352 E	22.56	351.3	33	5.0
43.	3	9	72	17	46	17.2	36.045 N	73.259 E	22.66	351.2	33	5.1
44.	3	9	72	20	32	18.4	35.921 N	73.499 E	22.5	351.6	33	5.2

(continued on next page)

Table 2 (*continued*)

S.	Date			Orig. Time			Location		Delta in deg.	Az in deg.	FD in km	M
N.	d	m	y	h	min	s						
45.	3	9	72	23	03	52.1	35.913 N	73.256 E	22.53	351.1	33	5.6
46.	4	9	72	00	14	10.0	35.920 N	73.365 E	22.52	351.3	55	5.5
47.	4	9	72	00	50	26.7	35.986 N	73.271 E	22.6	351.2	68	5.3
48.	4	9	72	01	23	49.5	35.801 N	73.314 E	22.41	351.2	33	5.4
49.	4	9	72	02	36	17.1	35.935 N	73.347 E	22.54	351.3	30	5.2
50.	4	9	72	03	51	20.9	35.926 N	73.456 E	22.51	351.5	35	5.3
51.	4	9	72	10	35	45.6	35.672 N	73.415 E	22.27	351.3	61	4.9
52.	4	9	72	13	37	51.4	35.797 N	73.301 E	22.41	351.2	33	5.2
53.	4	9	72	13	42	18.1	35.919 N	73.409 E	22.51	351.4	33	5.8
54.	5	9	72	04	07	27.0	35.865 N	73.412 E	22.46	351.4	33	5.0
55.	5	9	72	20	08	35.0	36.181 N	70.782 E	23.26	346.3	154	4.7
56.	7	9	72	02	54	58.3	2.050 S	68.009 E	18.15	211.7	33	5.8
57.	20	9	72	20	44	53.2	14.421 N	56.637 E	20.2	274.8	33	5.3
58.	21	9	72	00	10	13.3	2.981 N	96.146 E	21.29	118.1	33	5.2
59.	21	9	72	00	46	40.4	2.963 N	96.160 E	21.31	118.1	33	5.0
60.	25	9	72	11	30	17.8	9.828 N	93.943 E	16.59	101.3	33	5.3
61.	26	9	72	19	10	31.4	35.964 N	73.602 E	22.53	351.9	33	4.9
62.	27	9	72	00	08	29.9	30.308 N	101.672 E	27.86	49.4	33	5.0
63.	27	9	72	02	03	39.1	33.915 N	72.724 E	20.67	348.8	46	4.9
64.	27	9	72	09	18	08.4	36.115 N	73.416 E	22.7	351.5	33	5.1
65.	27	9	72	20	24	55.6	35.170 N	73.037 E	21.84	350.3	39	5.0
66.	28	9	72	09	00	38.0	5.712 S	105.517 E	33.85	122.8	33	5.4
67.	29	9	72	16	21	38.0	30.400 N	101.518 E	27.79	49.1	33	5.1
68.	29	9	72	20	24	42.0	30.275 N	101.673 E	27.84	49.5	33	5.1
69.	30	9	72	06	59	59.8	36.430 N	70.564 E	23.55	346.0	204	4.9
70.	6	10	72	20	22	03.2	3.274 N	98.522 E	23.22	114.4	124	5.3
71.	9	10	72	07	18	23.6	28.173 N	56.028 E	24.64	309.4	33	5.2
72.	12	10	72	00	21	14.2	35.918 N	73.329 E	22.52	351.3	49	5.2

$$W(K) = AK^{-P} \tag{14}$$

The index p may be changed with depth as well as the strength A. Thus, it provides a wide variety of models. A large number of models have been tried having uniform media down to a cutoff depth, but none of the fits were judged to be acceptable. A model of a two-overlapping-layer power-law medium was suggested (Flatte and Moody, 1990; Wu and Flatte, 1990; Tripathi and Ram, 1997) and the reliability of the model has been proved (Flatte et al., 1991).

A model consisting of a two-overlapping-layer (Fig. 5) power law medium has been obtained. The extension of the first layer is from the surface of the earth down to 160 km depth in which the heterogeneities are defined by Gaussian correlation function (power law index $p=0$). The second layer extends from 16 to 280 km depth in which the heterogeneities are defined by exponential correlation function (power law index $p=4$). Fig. 6 shows the comparison of the data and the obtained best model. The curves for shallow layer alone and deep layer alone are shown in Fig. 7. While the result of extending the bottom of the shallow layer to 280 km depth and the result of

extending the top of the deep layer to the surface instead of up to 16 km depth are shown in Fig. 8. It is clear from the Figs. 7 and 8 that the fits are inferior to the best model although the fits in Fig. 8 is not far from our best model.

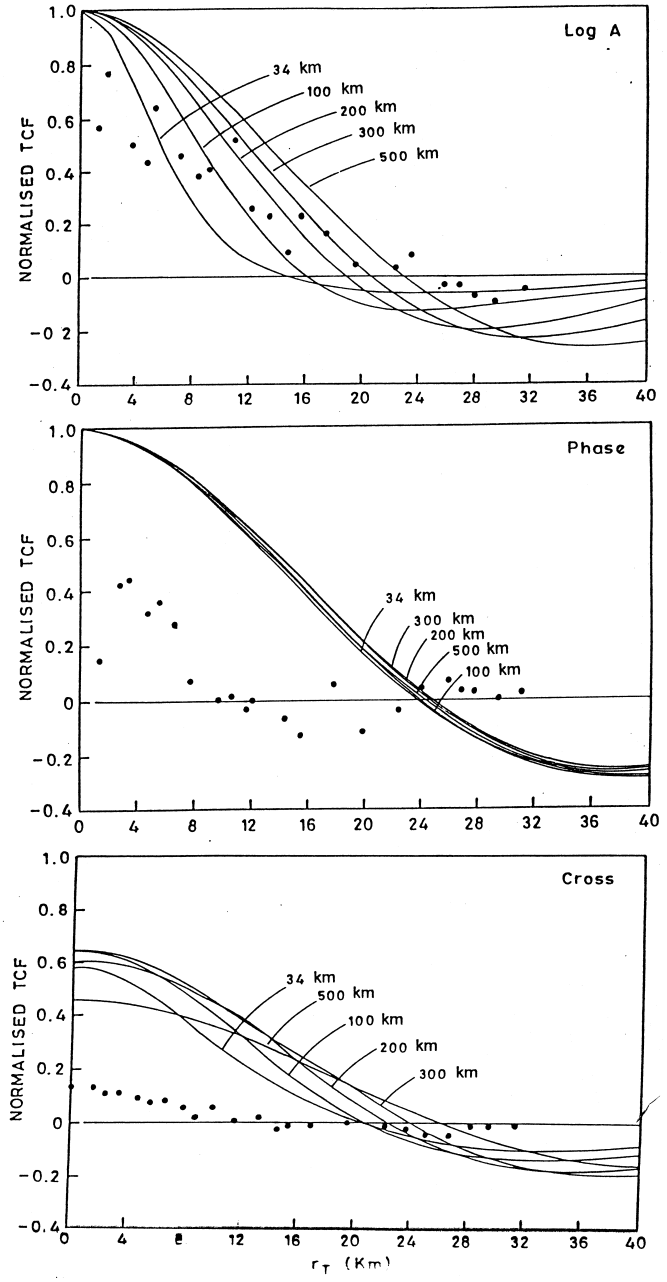

Fig. 4. A comparison between observed normalized TCFs for log-amplitude, phase and their cross coherence at the Gauribidanur Seismic Array (black circles) and theoretical curves based on uniform random medium with exponential correlation functions having a scale length of 18 km. The media extend from the surface to depths of 34–500 km.

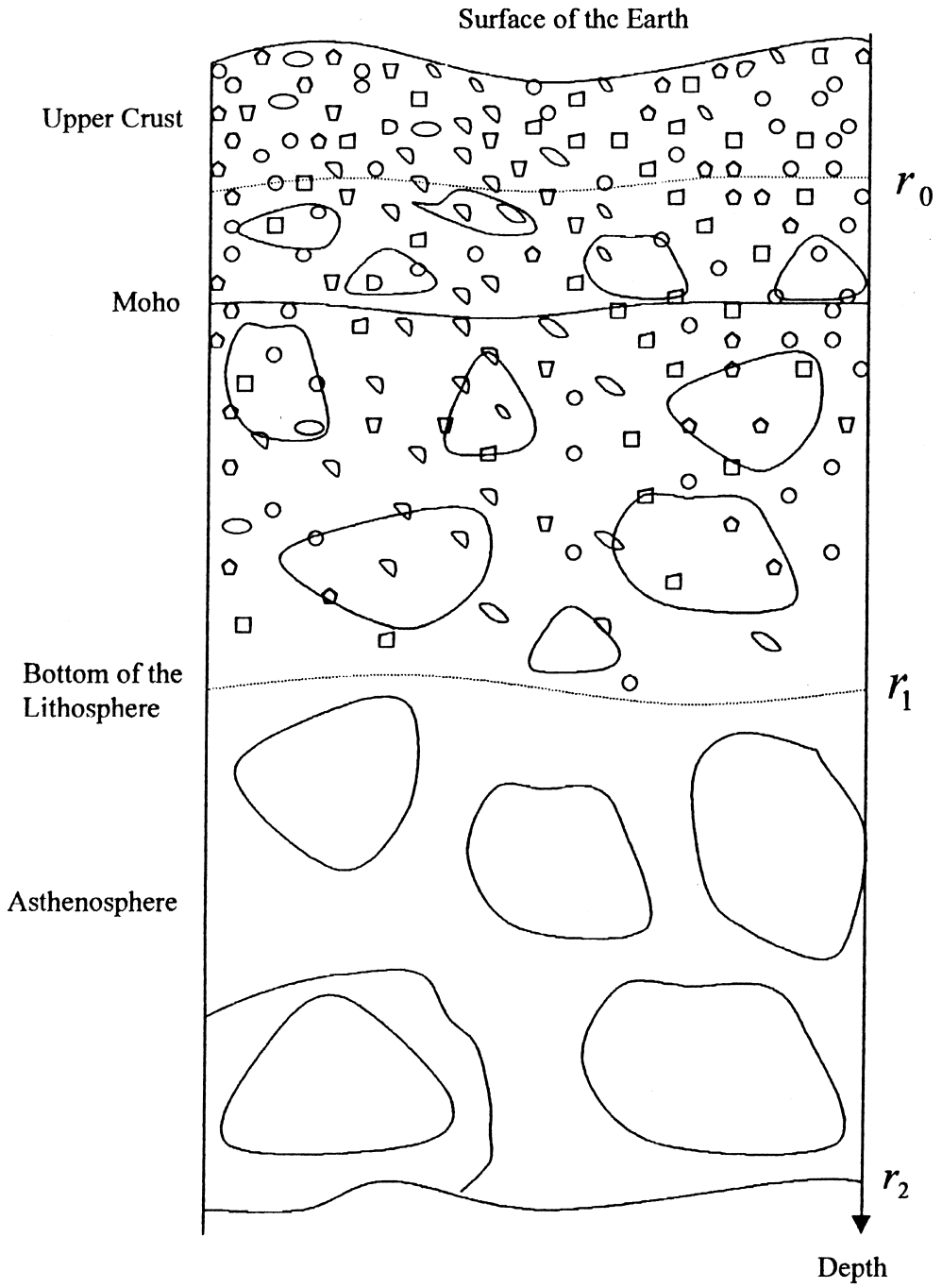

Fig. 5. A schematic representation of the best model for the random variations under the GBA. First layer is from the surface of the earth to r_1 and the second layer extends from r_0 to r_2.

In this model, the rms P-wave velocity variation is directly proportional to the rms variations in phase and log-amplitude. The observed values of rms of u and ϕ are 0.40 and 0.88, respectively. If the medium is considered to be isotropic, rms P-wave velocity variations of 0.8% in the upper

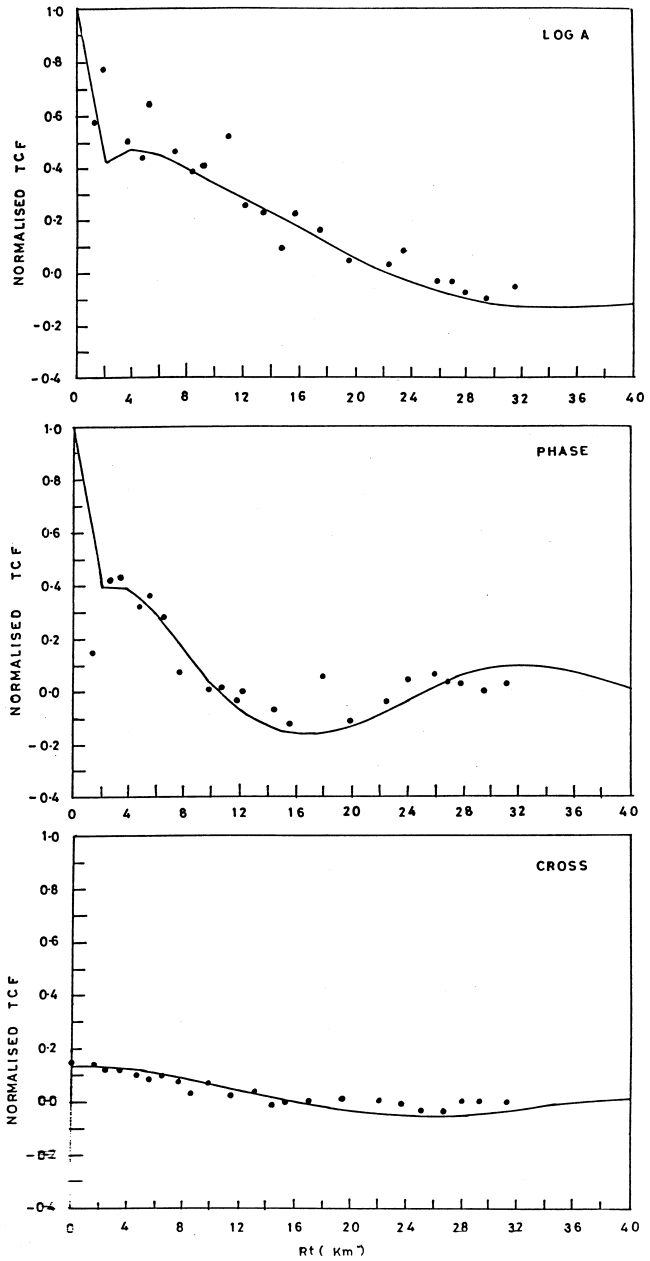

Fig. 6. A comparison between the observed data and the prediction of the best model, consisting of two overlapping layers. The first layer extends from surface to a depth of 160 km with power law index 0. The second layer extends from 16 km to 280 km depth with power law index 4 such that for the overlapping depth region, they have equal spectral levels at wave number 0.36 km^{-1}.

layer and 0.3% in the lower layer are implied from the estimated rms value of u. On the other hand, velocity variations in the upper and lower layers of 1.5 and 0.6%, respectively, were estimated when rms value of ϕ is taken into account. The difference between the values obtained from log-amplitude variance and from phase variance is not very significant because the determination

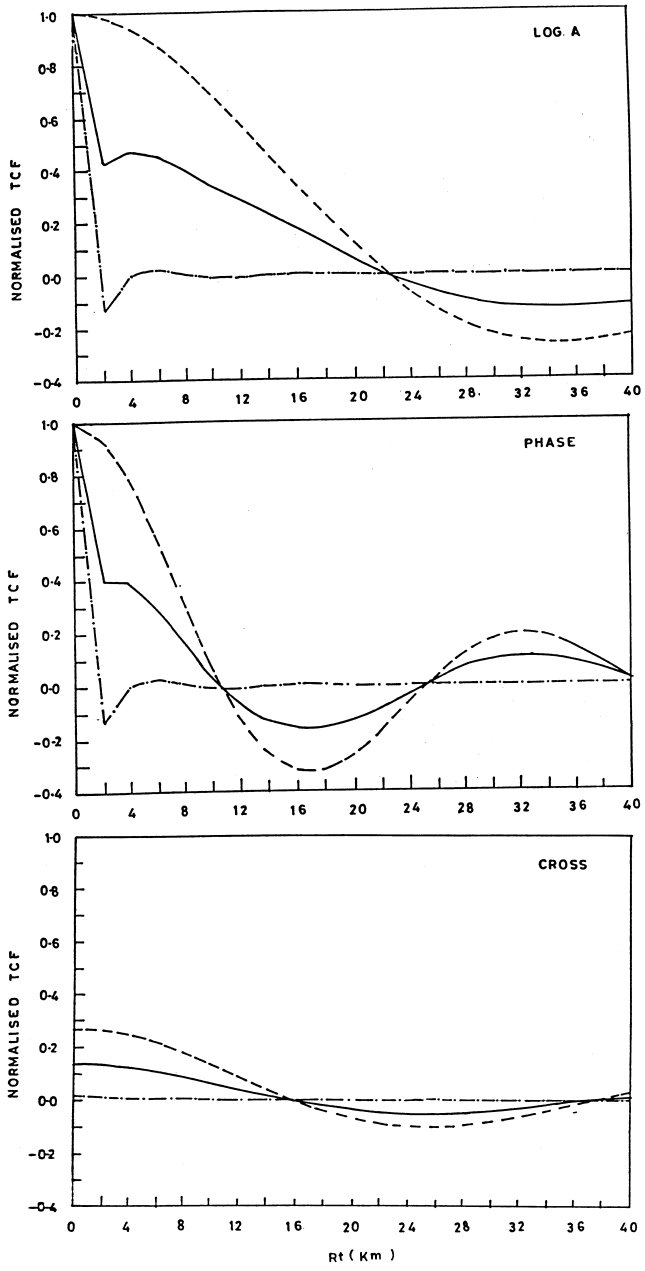

Fig. 7. A comparison between the best model curve (continuous line) and the predictions for variations taken from the model. The upper layer alone is shown by a small dashed line and the lower layer alone by a bigger dashed line with points.

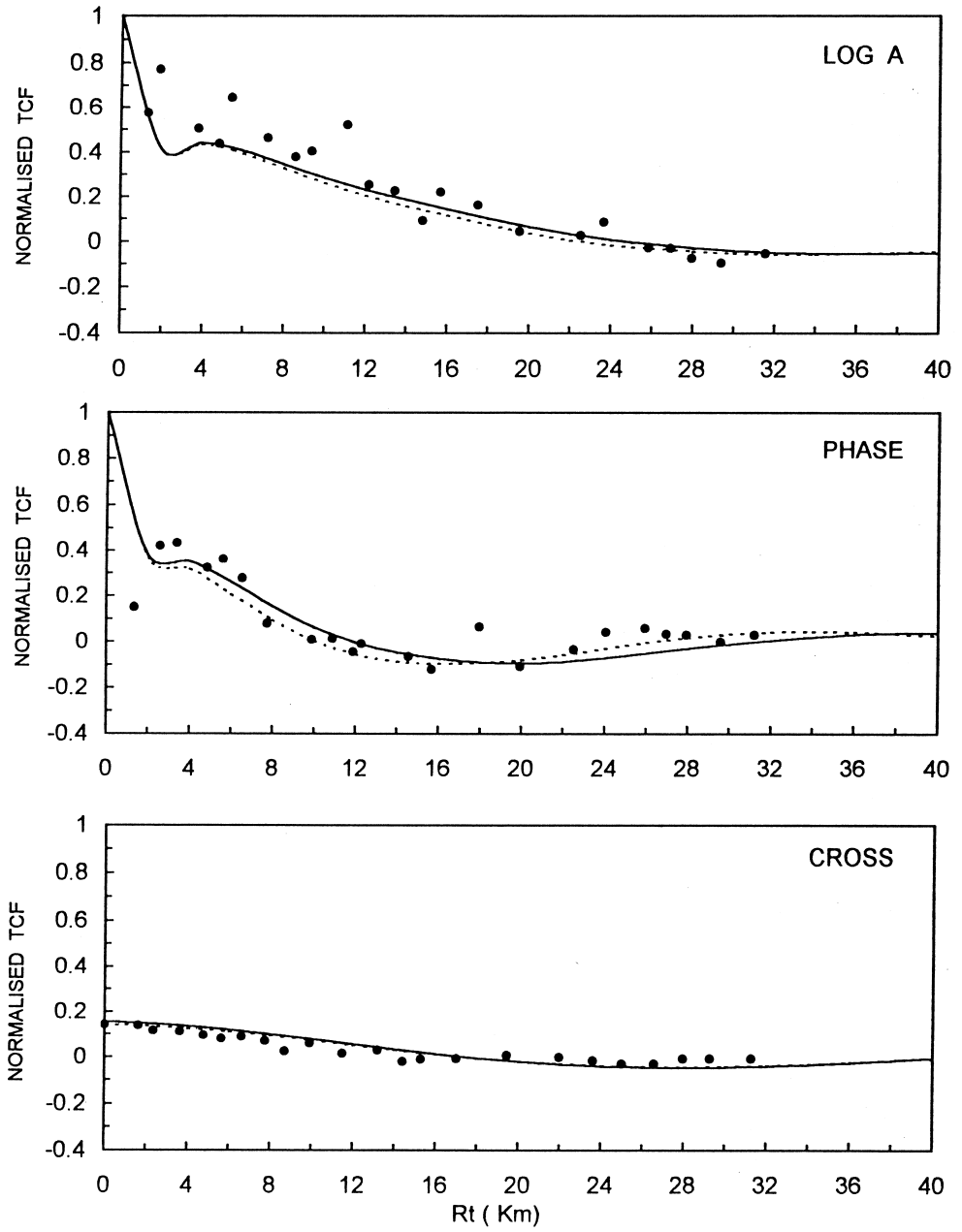

Fig. 8. A comparison between the data points and variation of the curves from the best model. The continuous line is for modification of the best model by extending the deep layer to the surface while the broken line is for extending the shallow layer to a depth of 280 km.

of over-all variance is difficult. The difference in the deduced values of rms *P*-wave velocity fluctuations indicates that large uncertainties are involved, i.e. rms *P*-wave velocity fluctuations is between 0.3 and 1.5%, if an isotropic medium is assumed.

5. Discussion and conclusions

Log-amplitude and phase transverse correlation functions (TCFs) were used previously but cross coherence of amplitude and phase TCF was not used until 1988 (Flatte and Wu, 1988). Approximate TCFs have been presented from LASA data showing a correlation length of the order of 10 km (Aki, 1973; Capon, 1974). The cross-coherence of log-amplitude and phase have been used as TCF for NORSAR (Flatte and Wu, 1988; Wu and Flatte, 1990). Here, the lithosphere and asthenosphere are characterized by random variations in the seismic wave speed of the earth and described by a spectrum, which may depend on depth and may be anisotropic.

A two-overlapping-layer model has been obtained. The extension of the first layer is from the surface of the earth to 160 km depth and that of the second layer from 16 to 280 km depth. The first layer is defined by Gaussian correlation function (power index $p=0$) while the second layer has the exponential correlation function (power index $p=4$) and a strength such that the $p=0$ and 4 spectra cross at $K=0.36$ km^{-1}.

The convection in the mantle is very complicated process. Within thin boundary layers at the top and bottom of the mantle may have most of the temperature increase with depth. But strong variations may occur in these boundary layers (Boss and Sacks, 1985; Olson et al., 1987). These variations may be of the spatial extent of the order 100 km and temperature difference up to 1000 K. Compositional differences and/or partial melting may be involved in the variations. Small-scale variations driven by dynamic mantle convection, or as fossilized compositional differences introduced by convection processes in earlier eras may be responsible for the earth's heterogeneities (Flatte and Wu, 1988). The presence of small-scale inhomogeneities in the shallow layer and predominance of large-scale inhomogeneities in the deep layer could be due to some change in rock strength and rock properties. Which may also be interpreted as a random distribution of relatively homogeneous layers with random discontinuities in *P*-wave speed from one layer to the next (Flatte and Wu, 1988).

The boundary between lithosphere and asthenosphere has been reported between 100 and 200 km with lateral variations of scale greater than 100 km beneath the southern Scandinavia (Husebye et al., 1986). The thickness of the top granitic layer is about 16 km (15.8 km) below GBA (Arora, 1971). Bhattacharya (1974) used the dispersion of Rayleigh and Love wave velocities in delineating the crust-mantle structure of the Indian peninsula and estimated about 5% decrease in S-wave velocity (4.55 km/s) in the layer 160–280 km depth as compared to the overlying and underlying layers. So the presence of a low velocity zone (LVZ) has been interpreted in this layer (Bhattacharya, 1974). Similar studies for the northwestern part of Indian peninsula (from Koyna to Shillong) also confirms the presence of LVZ from 140 to 340 km depth (Bhattacharya, 1991). Thus other studies have indicated structure at depth 180–260 km which should be combined with present observations.

The results can be interpreted as the 280 km may be the bottom of the thermal boundary layer in the mantle with the bottom of the lithosphere being 160 km. It has been concluded that the low velocity zone is present from 150 to 200 km in west Eurasia (Given and Helmberger, 1980) and from 200 to 250 km beneath NORSAR (Flatte and Wu, 1988). It is likely that a LVZ may be present from 160 to 280 km below the GBA array. A further refinement in the model may be possible by using the angular coherence functions of log-amplitude, phase and their cross-coherence. Though, in the present study, it is raw to have meaningful result about the mantle convec-

tion form this type of heterogeneity studies but at least it gives an indication about the introduction of the heterogeneity may be due to mantle convection. A detailed modelling of the mantle dynamics may give better result.

6. Uncited Reference

bib34 Wu, 1989 is not cited in text

Acknowledgements

The author is very much thankful to Professor H. Sato of Tohoku University, Japan; Professor W. Jacoby of Institut fur Geowissenschaften, Johannes Gutenberg-Universitat, Mainz and two anonymous reviewers for their valuable comments, which has significantly improved the paper. The author is also very much thankful to Professor Avadh Ram for reading the manuscript and making valuable suggestions and giving the GBA waveform data used in this study. Also, the author thankfully acknowledges the financial support by the Department of Science and Technology, New Delhi through grant No. HR/OY/A-14/96.

References

Aki, K., 1973. Scattering of P waves under the Montana LASA. J. Geophys. Res. 78, 1334–1346.
Aki, K., 1980. Scattering and attenuation of shear waves in the lithosphere. J. Geophys. Res. 85, 6496–6504.
Aki, K., 1981. Source and scattering effects on the spectra of small local earthquakes. Bull. Seismol. Soc. Am. 71, 1687–1700.
Aki, K., Chouet, B., 1975. Origin of coda waves: source, attenuation and scattering effects. J. Geophys. Res. 80, 3322–3342.
Arora, S.K., 1971. A study of the earth's crust near Gauribidanur in southern India. Bull. Seismol. Soc. Am. 61, 671–683.
Bergmann, P.G., 1946. Propagation of radiation in a medium with random inhomogeneities. Phys. Rev. 70, 486.
Berteussen, K.A., Christoffersson, A., Husebye, E.S., Dahle, A., 1975. Wave scattering theory in analysis of P-wave anomalies at NORSAR and LASA. Geophys. J.R. Astron. Soc. 42, 403–417.
Berteussen, K.A., Husebye, E.S., Mereu, R.F., Ram, A., 1977. Quantitative assessment of the crust — upper mantle heterogeneities beneath the Gauribidanur Seismic array in southern India. Earth Planet. Sci. Lett. 37, 326–332.
Bhattacharya, S.N., 1974. Crust-mantle structure of the Indian peninsula from surface wave dispersion. Geophys. J. R. Astron. Soc. 36, 373–383.
Bhattacharya, S.N., 1991. Surface wave and lithospheric structure across the northwestern part of the Indian peninsula. Pure and Appl. Geophys. 135, 53–59.
Boss, A.P., Sacks, I.S., 1985. Formation and growth of deep mantle plumes. Geophys. J.R. Astron. Soc. 80, 241–255.
Capon, J., 1974. Characterization of Crust and upper mantle medium. Bul. Seismol. Soc. Am. 64, 235–266.
Capon, J., Berteussen, K.A., 1974. A random medium analysis of crust and upper mantle structure under NORSAR. Geophys. Res. Lett. 1, 327–328.
Chernov, L.A., 1960. Wave Propagation in a Random Medium. McGraw Hill, New York.
Fante, R.L., 1980. Electromagnetic beam propagation in turbulent media: an update. Proc. IEEE 68, 1424–1443.
Flatte, S.M., Wu, R.S., 1988. Small-Scale structure in the Lithosphere and Asthenosphere deduced from arrival time and amplitude fluctuations at NORSAR. J. Geophys. Res. 93, 6601–6614.

Flatte, S.M., Moody, T.N., 1990. Weak-fluctuation theory via path integrals. Contribution No. 106 of the Institute of Tectonics of the University of California, Santa Cruz.

Flatte, S.M., Dashen, R., Munk, W.H., Watson, K.M., Zachariasen, F., 1979. Sound Transmission Through a Fluctuating Ocean. Cambridge University Press, New York.

Flatte, S.M., Wu, R.S., Shen, Z.K., 1991. Nonlinear inversion of phase and amplitude coherence functions at NORSAR for a model of uniform heterogeneities. Geophys. Res. Lett. 18, 1269–1272.

Given, J.W., Helmberger, D.V., 1980. Upper mantle structure of northwestern Eurasia. J. Geophys. Res. 85, 7183–7194.

Husebye, E.S., Hovland, J., Christoffersson, A., Astrom, K., Slunga, R., Lund, C.E., 1986. Tomographical mapping of the lithosphere and asthenosphere beneath southern Scandinavia and adjacent areas. Tectonophysics 128, 229–250.

Ishimaru, A., 1977. Theory and application of wave propagation and scattering in random media. J. Proc. IEEE 65, 1030–1061.

Mintzer, D., 1953. Wave propagation in a randomly inhomogeneous medium. J. Acoust. Soc. Am. 25, 922–927.

Munk, W.H., Zachariasen, F., 1976. Sound propagation through a fluctuating ocean — theory and observation. J. Acoust. Soc. Am. 59, 818–838.

Olson, P., Schubert, G., Anderson, C., 1987. Plume formation in the D″-layer and the roughness of the core-mantle boundary. Nature 327, 409–413.

Powell, C.A., Meltzer, A.S., 1984. Scattering of P waves beneath SCARLET in southern California. Geophys. Res. Lett. 11, 481–484.

Prokhorov, A.M., Bunkin, F.V., Gochelashvity, K.S., Shishov, V.I., 1975. Laser irradiance propagation in turbulent media. Proc. IEEE 63, 790–811.

Sato, H., 1982. Attenuation of S waves in the lithosphere due to scattering by its random velocity structure. J. Geophys. Res. 87, 7779–7785.

Strohbehn, J.W. (Ed.), 1978. Laser Beam Propagation in the Atmosphere. Springer-Verlag, New York.

Tatarskii, V.I., 1971. The Effects of the Turbulent Atmosphere on Wave Propagation. National Technical Information Service, Springfield, VA.

Tatarskii, V.I., Zavorotnyi, V.U., 1980. Strong fluctuations in the light propagation in a randomly inhomogeneous medium. Progr. Opt. 18, 204–256.

Tripathi, J.N., Ram, A., 1996. Estimation of velocity perturbations using amplitude and phase fluctuations for earthquakes recorded at Gauribidanur seismic array in southern India. Acta Geodaetica et Geophysica Hungarica 31 (1–2), 126–144.

Tripathi, J.N., Ram, A., 1997. Elastic wave scattering in a Randium media characterized by von-Karman correlation function and small-scale inhomogeneities in the lithosphere. Geophys. J. Int. 131, 682–698.

Wu, R.S., 1982. Attenuation of short period seismic waves due to scattering. Geophys. Res. Lett. 9, 9–12.

Wu, R.S., Aki, K., 1985a. Elastic wave scattering by a random medium and the small-scale Inhomogeneities in the lithosphere. J. Geophys. Res. 90, 10261–10273.

Wu, R.S., Aki, K., 1985b. Scattering characteristic of elastic waves by an elastic heterogeneity. Geophysics 50, 582–595.

Wu, R.S., Aki, K., 1985c. The fractal nature of the inhomogeneities in the lithosphere evidenced from seismic wave scattering. Pure Appl Geophys. 123, 805–808, 18.

Wu, R.S., Flatte, S.M., 1990. Transmission fluctuation across an array and heterogeneities in the crust and upper mantle. Pure Appl. Geophys. 132, 175–196.